Electronic Supplementary Information

Hybrid octahedral Au nanocrystals and Ag nanohole arrays as substrate for highly sensitive and reproducible surface-enhanced Raman scattering

Tiancheng Gong, ‡[a] Yunfei Luo, ‡[ac] Haibin Zhang, ‡[bc] Chengwei Zhao, [ac] Weisheng Yue, [a] Mingbo Pu, [a] Weijie Kong, [a] Changtao Wang, [a] and Xiangang Luo *[a]

[a] *State Key Laboratory of Optical Technologies on Nano-Fabrication and Micro-Engineering, Institute of Optics and Electronics, Chinese Academy of Sciences, P.O. Box 350, Chengdu 610209, China*

[b] *Lightweight Optics and Advanced Materials Center, Institute of Optics and Electronics, Chinese Academy of Sciences, P.O. Box 350, Chengdu 610209, China*

[c] *University of Chinese Academy of Sciences, Beijing 100049, China*

‡ *Contributed equally to this work*
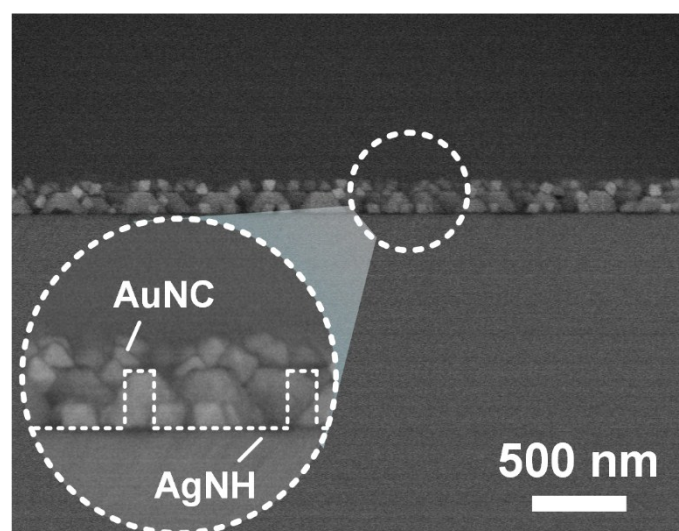
1. Side-view SEM image of AuNC-AgNH

Fig. S1 The side-view SEM image of AuNC-AgNH.

* Corresponding author. E-mail: lxg@ioe.ac.cn (X. Luo).

2. Raman spectrum of solid 4-Mpy

The Raman spectrum of solid 4-Mpy was measured with a 100× objective and integration times of 5 s, using an excitation wavelength of 785 nm. The result is shown in Fig. S2. Compared with the Raman spectrum of solid 4-Mpy and 4-Mpy molecules adsorbed on SERS substrate in Fig. 3 in the manuscript, the vibration mode of ring breathing can be observed for bulk 4-Mpy at 988 cm^{-1} and is blue-shifted to 1005 cm^{-1} in the SERS spectra due to the variation of hydrogen bonds when the Au atoms are in the same plane with the 4-MPy molecules [S1, S2]. The vibration mode of trigonal ring-breathing with C=S can be observed for bulk 4-Mpy at 1104 cm^{-1} and is red-shifted to 1098 cm^{-1} in the SERS spectra due to the coupling of the ring-breathing mode with the C=S stretching when sulfur is bonded to the Au surface [S2].
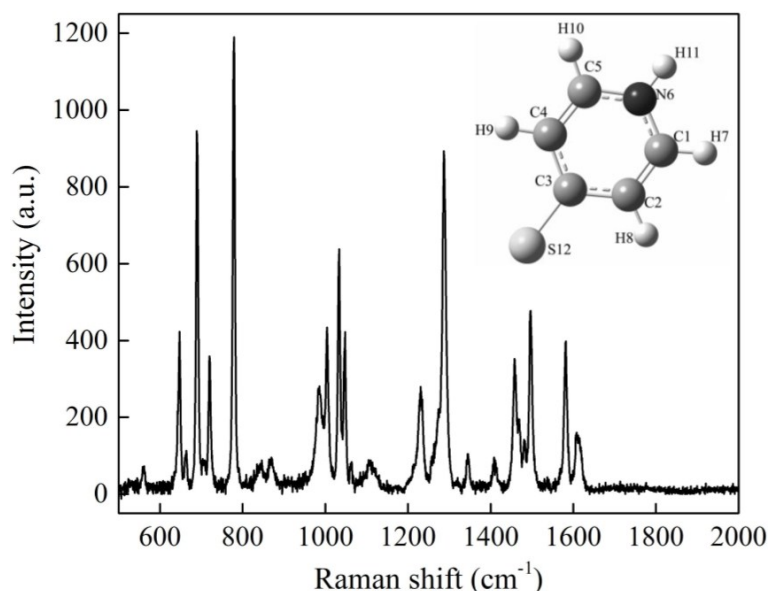

Fig. S2 Raman spectrum of solid 4-Mpy. Inset shows the configuration of 4-Mpy [S1].

3. Calculation of the EFs

Before the calculation of EFs, we should estimate the surface area within the laser spot for each samples. From the SEM image in Fig. 3(b), we can see that the quantity of AgNHs is ~33 within the laser spot and the surface area of AgNHs is equal to the area of laser spot, which is ~3.14 μm^2. The surface area of AuNCs and AuNC-AgNH can be estimated by the total surface area of octahedral AuNCs within the laser spot. We have counted the quantity of AuNCs within the white dashed circles and there are ~624 and ~588 particles in Fig. 3(a) and (b), respectively.

We should note that in Fig. 3(b), AuNCs at the bottom of AgNHs could not be identified effectively and there is at least one AuNC at the bottom of AgNHs. Therefore the estimated quantity of AuNCs in the hybrid structure is ~588 + 33 = ~621. In general, all faces of an octahedral AuNC are capable of adsorbing molecules [S3], so the effective surface area on a single AuNC is ~0.0195 μm^2, and the effective surface area within the laser spot (S_{SERS}) of AuNCs and AuNC-AgNH are 12.17 and 12.11 μm^2, respectively. We have provided a complete calculation process of the EF values below, using AuNC-AgNH @1098 cm^{-1} as an example:

- I_{SERS} can be obtained by the Raman spectrum of 4-Mpy on AuNC-AgNH in Fig. 3(c) in the manuscript, and the value @1098 cm^{-1} is ~18328.12 counts.

- N_{bulk} can be estimated by the volume of the laser waist (V_{laser}) and the density of solid samples (ρ_{solid}). V_{laser} can be obtained by the focus depth (h_{focus}) and the area (S_{laser}) of laser spot. From reference [S4], we can obtain that h_{focus} of 785 nm laser is ~10 μm, and S_{laser} of laser spot with a diameter of 2 μm is ~3.14 μm^2, thus $V_{laser} = S_{laser} \times h_{focus} = 31.4$ μm^3. From reference [S5], we can obtain that ρ_{solid} of the solid 4-Mpy is 1.2 g/cm^3. Therefore, the mass of the solid 4-Mpy (m_{solid}) with in the volume of the laser waist can be calculated by $m_{solid} = \rho_{solid} \times V_{laser} = 3.768 \times 10^{-11}$ g. The molar mass of 4-Mpy (M_{4-Mpy}) is 79.1 g/mol and $N_A = {\sim}6.02 \times 10^{23}$ is the avogadro's constant. Finally, N_{bulk} can be calculated by $N_{bulk} = m_{solid}/M_{4-Mpy} \times N_A = {\sim}2.87 \times 10^{11}$.

- I_{bulk} can be obtained by the Raman spectra of the solid 4-Mpy in Fig. S2, and the value @1098 cm^{-1} is ~17.92 counts.

- N_{SERS} can be estimated by assuming monolayer coverage of 4-Mpy molecules on the surface of SERS substrate. From reference [S6], a packing density ($\rho_{molecule}$) of 6.8×10^{14} molecules/cm^2 was used for calculation. Thus $N_{SERS} = \rho_{molecule} \times S_{SERS} = {\sim}8.23 \times 10^7$.

- $EF = (I_{SERS} \times N_{bulk})/ (I_{bulk} \times N_{SERS}) = {\sim}3.6 \times 10^6$.

4. Size optimization of AuNCs and AgNHs

Firstly, we simulated the electric field distributions of AuNCs with edge length of 65, 75, 85 and 95 nm, respectively, and the gap between two adjacent AuNCs was set to 5 nm. The simulation results are shown in Fig. S3. Fig. S3(a)~(d) show the electric field distributions of AuNCs with different edge length. An obvious "hotspots" effect can be observed between two

adjacent AuNCs in each figure, which mainly determined the EM enhancement of SERS substrates. In order to make a quantitative analysis of the EM enhancement, we extracted the field distributions in the area of hotspots in each figure under the white dashed lines in Fig. S3(a)~(d) and the results are shown in Fig. S3(e). From the results we can see that the maximum field intensities are 9.3, 10.4, 10.5 and 10.2 V/m with the edge length of 65, 75, 85 and 95 nm, respectively, which has a trend of firstly increase and then decrease with the increasing of edge length. Besides, the simulation results indicate that AuNCs with the edge length of 75 and 85 nm can achieve higher EM enhancement than the other two sizes.
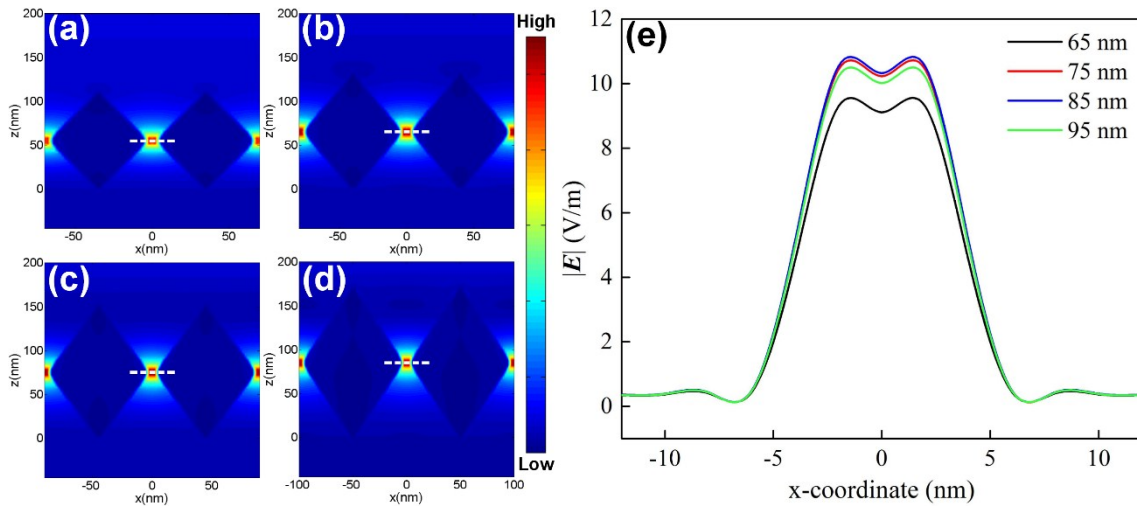

Fig. S3 The electric field distributions of AuNCs with edge length of (a) 65, (b) 75, (c) 85 and (d) 95 nm. (e) The corresponding electric field distributions under the white dashed lines in (a)~(d).

Secondly, we simulated the electric field distributions of AuNC-AgNH with different sizes. The edge length of AuNCs were set as 75 and 85 nm, respectively, and the gap between two adjacent AuNCs was set to 5 nm, therefore the corresponding diameter of AgNHs were set to 240 and 270 nm, respectively. Fig. R4(a) and (b) show the field distributions of AuNC-AgNH with edge length of 75 and 85 nm in the X-Z plane through the center of nanoholes ($y = 0$), respectively. Fig. S4(c) shows the corresponding field distributions under the white dashed lines in Fig. S4(a) and (b). From the simulation results we can see that the combination of AuNCs with edge length of 75 nm and AgNHs with diameter of 240 nm can achieve better EM enhancement, and the maximum field intensity of 33.3 V/m can be observed at the gap between AuNCs and the side of AgNHs, which is ~1.6 times higher than AuNCs with edge length of 85
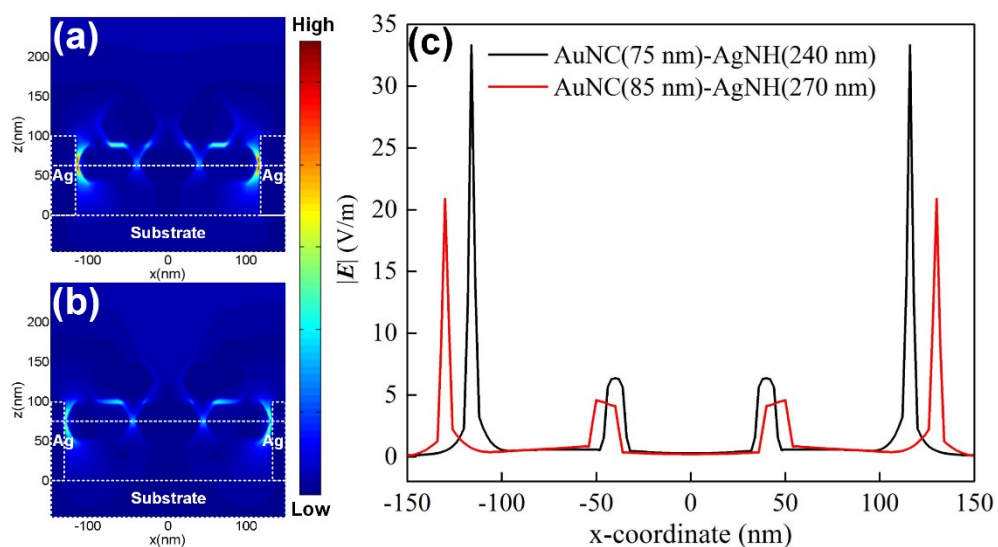
nm and AgNHs with diameter of 270 nm.

Fig. S4 The electric field distributions of AuNC-AgNH with edge length of (a) 75 and (b) 85 nm in the X-Z plane through the center of nanoholes (y = 0). (c) The electric field distributions of AuNC-AgNH with different size under the white dashed lines in (a) and (b).

Based on the preliminary optimization of the sizes of AuNC-AgNH by simulation, we fabricated the hybrid structure of AuNCs with edge length of 75 nm and AgNHs with diameter of 240 nm and used in the Raman experiments.

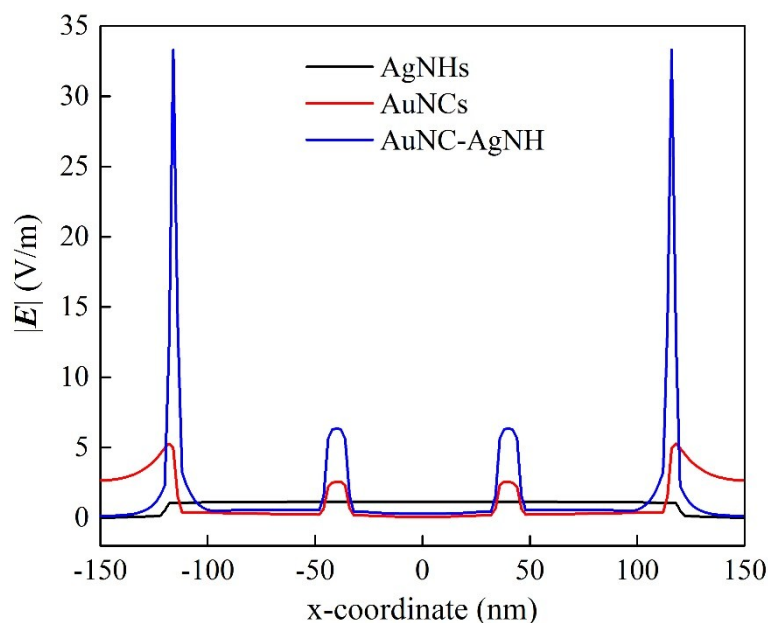**5. The electric field distributions under the blue dashed lines**

Fig. S5 The electric field distributions of AgNHs, AuNCs and AuNC-AgNH under the blue dashed lines in Fig. 4(a1), (b1) and (c1) in the manuscript.

References

[S1] L. Zhang, Y. Bai, Z. Shang, Y. Zhang and Y. Mo, J. Raman Spectrosc., 2007, 38, 1106–1111.

[S2] Q. Yu, P. Guan, D. Qin, G. Golden and P. M. Wallace, Nano Lett., 2008, 8, 1923–1928.

[S3] H.-L. Wu, H.-R. Tsai, Y.-T. Hung, K.-U. Lao, C.-W. Liao, P.-J. Chung, J.-S. Huang, I-C. Chen and M. H. Huang, Inorg. Chem., 2011, 50, 8106–8111.

[S4] C. Muehlethaler, C. R. Considine, V. Menon, W.-C. Lin, Y.-H. Lee and J. R. Lombardi, ACS Photonics, 2016, 3, 1164–1169.

[S5] W. Yue, Z. Wang, J. Whittaker, F. Lopez-royo, Y. Yang and A. V. Zayats, J. Mater. Chem. C, 2017, 5, 4075–4084.

[S6] A. D. McFarland, M. A. Young, J. A. Dieringer and R. P. Van Duyne, J. Phys. Chem. B, 2005, 109, 11279.